

Energy transport in a one-dimensional harmonic ternary chain with Ornstein–Uhlenbeck disorder

This article has been downloaded from IOPscience. Please scroll down to see the full text article.

2012 J. Phys.: Condens. Matter 24 495401

(<http://iopscience.iop.org/0953-8984/24/49/495401>)

View [the table of contents for this issue](#), or go to the [journal homepage](#) for more

Download details:

IP Address: 187.41.57.126

The article was downloaded on 17/11/2012 at 15:44

Please note that [terms and conditions apply](#).

Energy transport in a one-dimensional harmonic ternary chain with Ornstein–Uhlenbeck disorder

M O Sales¹, S S Albuquerque² and F A B F de Moura¹

¹ Instituto de Física, Universidade Federal de Alagoas, Maceió, AL 57072-970, Brazil

² Curso de Física, Universidade Federal de Alagoas Campus Arapiraca, Av. Manoel Severino Barbosa, s/n, Bom Sucesso, Arapiraca, AL, CEP: 57309-005, Brazil

E-mail: fidelis@fis.ufal.br

Received 24 July 2012, in final form 11 October 2012

Published 12 November 2012

Online at stacks.iop.org/JPhysCM/24/495401

Abstract

In this paper we study a one-dimensional ternary harmonic chain with the mass distribution constructed from an Ornstein–Uhlenbeck process. We generate a ternary mass disordered distribution by generating the correlated Ornstein–Uhlenbeck process and mapping it into a sequence of three different values. The probability of each value is controlled by a fixed parameter b . We analyze the localization aspect of the above model by numerical solution of the Hamilton equations and by the transfer matrix formalism. Our results indicate that the correlated ternary mass distribution does not promote the appearance of new extended modes. In good agreement with previous work, we obtain extended modes for $b \rightarrow \infty$; however, we explain in detail the main issue behind this apparent localization–delocalization transition. In addition, we obtain the energy dynamics for this classical chain.

1. Introduction

The energy transport in nonperiodic classical chains is a very interesting issue with several lines of investigation [1–21]. The key ingredient behind the energy flux in low-dimensional nonperiodic classical lattices is the nature of the vibrational modes. The vibrational eigenstates of a one-dimensional disordered harmonic chain with N random masses can be mapped onto a one-electron tight-binding model [1]. It has been demonstrated that most of the normal vibrational modes are localized and there are few low-frequency modes which are not localized, whose number is of the order of \sqrt{N} [1, 14]. Furthermore, by using analytical arguments, it has also been shown that the transport of energy in mass disordered harmonic chains is strongly dependent on the non-scattered vibrational modes as well as the initial excitation [15]. Calculations have indicated that uncorrelated random chains have a super-diffusive behavior for the second moment of the energy distribution ($M_2(t) \propto t^{1.5}$) for impulse initial excitations, while for initial displacement excitations a sub-diffusive spread takes place ($M_2(t) \propto t^{0.5}$). The dependence of the second moment spread on

the initial excitation was also obtained in [22]. Within this context, [16–20] have demonstrated that this framework can change if some correlations are introduced in the disorder distribution. It was obtained that besides these low-frequency extended modes, a new set of high-frequency non-scattered modes can be found if short- [16, 17] or long-range correlations [18–20] in the disorder distribution (spring constants or masses) are considered. In fact, in [18] a study was presented of the nature of the collective vibrational modes in harmonic chains with long-range correlated random masses, with spectral power density $S \propto k^{-\alpha}$. By using the transfer matrix the emergence of a phase of low-energy extended collective excitations in the strong correlation regime ($\alpha > 1$) was observed. Moreover, the authors found that the energy second moment $M_2(t)$ displays a crossover from an anomalous sub-diffusive or super-diffusive regime (depending on the initial displacement or impulse excitation, respectively) to an asymptotic ballistic behavior.

Previous work on the transport properties in systems with correlated disorder has been carried out by considering the disorder distribution uniformly chosen in a finite range [W_1, W_2]. Within the context of one electron in a disordered

chain some authors have considered models where the on-site energy can assume two or three different values i.e., the binary and ternary models respectively [23, 24]. In particular, the Anderson model with long-range correlated disorder chosen as a ternary sequence was studied in [24]. In the case of the on-site energy distribution generated as an uncorrelated random sequence, the system is naturally an insulator. However, the authors have shown that, if a long-range correlated ternary on-site energy distribution is considered, an Anderson localization–delocalization phase transition can be observed [24]. More recently, the effect of long-range correlations in the random ternary sequence of capacitances of a classical transmission line (TL) has been studied by Lazo and Diez [25, 26]. To generate the ternary correlated distribution the Fourier filtering method [25] and the Ornstein–Uhlenbeck (OU) process [26] were used. In both cases a transition was observed from the non-conducting to the conducting state of the TL induced by strong correlations.

In this paper we will study the energy transport in a harmonic chain with correlated disorder distribution. Here, we study a one-dimensional ternary harmonic chain with the mass distribution constructed from an Ornstein–Uhlenbeck process. We generate a ternary mass disordered distribution by generating the correlated Ornstein–Uhlenbeck process and mapping it into a sequence of three different values. The probability of each value is controlled by a fixed parameter b . In that way, we will generate a ternary mass distribution with long-range correlations. We analyze the localization aspect of the above model by numerical solution of the Hamilton equations and by the transfer matrix formalism. Our results indicate that the correlated ternary mass distribution does not promote the appearance of new extended modes. In good agreement with previous work, we obtain extended modes for $b \rightarrow \infty$; however, by using a numerical calculation of the local strength of disorder, we will explain in detail the nature of the phase transition found here. In addition, we obtain the energy dynamics for this classical chain.

2. Model and formalism

We start by considering a harmonic chain of N masses, for which the equation of motion for the displacements $q_n = u_n \exp i\omega t$ with vibrational frequency ω is [14, 16]

$$(\eta_{n-1} + \eta_n - \omega^2 m_n)u_n = \eta_{n-1}u_{n-1} + \eta_n u_{n+1}. \quad (1)$$

In our calculations, we will use units such that all elastic force couplings $\eta_n = 1$, and the random site masses m_n will be taken from an Ornstein–Uhlenbeck (OU) process [26]. The OU process is defined by the stochastic differential equation

$$\frac{dx}{dt} = -\gamma x(t) + \sqrt{C}\beta(t), \quad (2)$$

where γ is the viscosity coefficient, C is the diffusion coefficient and $\beta(t)$ is the stochastic term [26]. $\beta(t)$ is a Gaussian white noise generated by the Box–Muller process with the following properties: $\langle \beta(t) \rangle = 0$ and $\langle \beta(t)\beta(t+\tau) \rangle = \delta(\tau)$. This stochastic process contains correlation between each step defined by $\langle x(t)x(t+\tau) \rangle = \frac{C}{2\gamma}e^{-\gamma\tau}$ [26]. In order to

generate the diagonal disorder from the OU process we will consider the numerical formalism obtained in [27] based on the discrete version of equation (2). In the discrete form, $x(t)$ is written as x_n , where n denotes the time step number ($t = n\Delta t$). Therefore, the discrete form of equation (2) is given by [27]

$$x_{n+1} = (e^{-\gamma\Delta t})x_n + \left[\sqrt{\frac{C}{2\gamma}(1 - e^{-2\gamma\Delta t})} \right] \beta_n. \quad (3)$$

Using the Box–Muller algorithm we calculate β_n in the following way:

$$\beta_n = \left(\sqrt{2 \ln \frac{1}{r_n}} \right) \cos 2\pi a_n, \quad (4)$$

where r_n and a_n are uniform random numbers defined in the interval $[0, 1]$. In addition, we normalize the sequence x_n to impose zero average and keep the variance equal to unity. Following [26], we will consider $C = \gamma^2$ and, therefore, the degree of correlation of the OU process becomes controlled by a single parameter γ . For $\gamma \rightarrow \infty$ the OU sequence evolves into the Gaussian white noise. For $\gamma \rightarrow 0$ the degree of correlation within the stochastic sequence increases. In [27, 26] it was shown that the OU sequence exhibits a spectral power density $S(f) \propto 1/f^2$ for $\gamma \rightarrow 0$. Using the normalized sequence x_n generated by the OU process, we will construct a ternary mass distribution as follows:

$$m_n = \begin{cases} 0.5 & \text{if } x_n < -b, \\ 1.0 & \text{if } -b \leq x_n \leq b, \\ 1.5 & \text{if } x_n > b, \end{cases} \quad (5)$$

where $b > 0$ controls the probability of each possible value of the mass value. We would like to emphasize the meanings of the two tunable parameters γ and b . The first one controls the degree of correlation in the disorder distribution considered, i.e., the Ornstein–Uhlenbeck process. For sufficiently small γ we are dealing with a strongly correlated disordered sequence. On the other hand, the b parameter defines the specificities of the mapping that we have used in the generation, from the OU process, of a discrete mass disordered sequence. For $b = 0$ we will map the OU process in a binary random sequence of two masses. For $b \rightarrow \infty$ we will deal with an ordered sequence of identical masses. We are interested in studying in detail the roles played by both parameters on the localization aspects and energy dynamics of harmonic chains. We should stress again that some authors have obtained an Anderson localization–delocalization phase transition in low-dimensional systems with OU disorder at the limit of $\gamma \rightarrow 0$ and $b > 4$ [24–26]. We are interested in studying this possibility within the context of a harmonic chain.

2.1. Localization properties

To reveal the degree of localization we will use the localization length λ . The best numerical method for accurately computing localization lengths in nonperiodic systems is the transfer matrix method (TMM). The TMM

is obtained by using a matrix recursive reformulation of the scaled displacement equation (equation (1))

$$\begin{pmatrix} u_{n+1} \\ u_n \end{pmatrix} = \begin{pmatrix} 2 - m_n \omega^2 & -1 \\ 1 & 0 \end{pmatrix} \begin{pmatrix} u_n \\ u_{n-1} \end{pmatrix}. \quad (6)$$

For a specific frequency ω , a 2×2 transfer matrix T_n connects the displacements at the sites $n - 1$ and n to those at the site $n + 1$,

$$T_n = \begin{pmatrix} 2 - m_n \omega^2 & -1 \\ 1 & 0 \end{pmatrix}. \quad (7)$$

Once the initial values for u_0 and u_1 are known, the value of u_n can be obtained by repeated iterations along the chain, as described by the product of transfer matrices

$$Q_N = \prod_{n=1}^N T_n. \quad (8)$$

The localization length of each vibrational mode is defined by [14, 16]

$$\lambda = \left\{ \lim_{N \rightarrow \infty} \frac{1}{N} \log \frac{|Q_N c(0)|}{|c(0)|} \right\}^{-1}, \quad (9)$$

where $c(0) = \begin{pmatrix} u_1 \\ u_0 \end{pmatrix}$ is a generic initial condition. Typically, 10^8 matrix products were used to calculate the localization length.

2.2. Energy transport

In order to study the time evolution of an initially localized energy pulse, we calculate the second moment of the energy distribution [15, 22]. This quantity is related to the thermal conductivity by Kubo's formula [15]. The classical Hamiltonian H for a harmonic chain can be written as

$$H = \sum_{n=1}^N h_n(t), \quad (10)$$

where the energy $h_n(t)$ at site n is given by

$$h_n(t) = \frac{P_n^2}{2m_n} + \frac{1}{4}[(Q_{n+1} - Q_n)^2 + (Q_n - Q_{n-1})^2]. \quad (11)$$

Here P_n and Q_n define the momentum and displacement of the mass at the n th site. The fraction of the total energy H at site n is given by $h_n(t)/H$ and the second moment of the energy distribution, $M_2(t)$, is defined by [15]

$$M_2(t) = \sum_{n=1}^N (n - n_0)^2 [h_n(t)/H], \quad (12)$$

where an initial excitation is introduced at the site n_0 at $t = 0$. Using the eighth-order Runge–Kutta method, we solve the Hamilton equations for $P_n(t)$ and $Q_n(t)$ and calculate $M_2(t)$. The second moment of the energy distribution, $M_2(t)$, has the same status as the mean-square displacement of the wave-packet of an electron in a solid [15, 22].

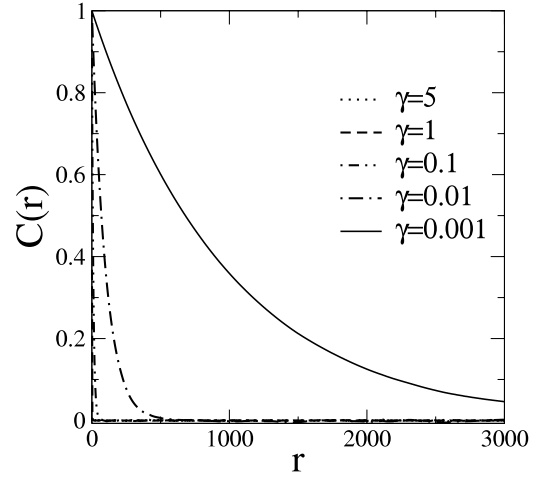


Figure 1. Numerical calculation of the two-point autocorrelation function defined by $C(r) = [1/(N - r)] \sum_{n=1}^{N-r} x_n x_{n+r}$. We can see that as γ is decreased the Ornstein–Uhlenbeck (OU) process displays an increasing of degree of correlation.

3. Results

3.1. Localization properties

Initially, to compare some statistical properties of the Ornstein–Uhlenbeck (OU) distribution, we compute the autocorrelation function ($C(r) = [1/(N - r)] \sum_{n=1}^{N-r} x_n x_{n+r}$) of the sequence $\{x_n\}$ (see figure 1). We can see clearly that the correlation function decays more slowly when γ is decreased. For $\gamma \gg 0$ we recover an uncorrelated random process. In order to calculate the typical localization length of the eigenstates, we use the transfer matrix technique for a long chain with N masses ($N \approx 10^8$). In this method, the self-averaging effect automatically takes care of statistical fluctuations. We estimate and control these fluctuations by following the deviations of the calculated eigenvalues of two adjacent iterations. Our data have statistical errors of less than 2%. In figures 2(a) and (b) we show data for the localization length λ versus the squared frequency ω^2 for a harmonic chain with OU mass disordered distribution with $\gamma = 1$ and 5 and $b = 0.25, 0.5, 0.75$ and 1. All calculations were averaged over 100 disorder configurations. For $\gamma = 1$ and 5 the localization length scales in proportion to the system size only for $\omega = 0$. For $\gamma \gg 0$ we obtained results compatible with a standard uncorrelated random harmonic chain. In figures 2(c)–(e) we show results for the localization length λ versus the squared frequency ω^2 for a harmonic chain with OU mass disordered distribution with $\gamma = 0.1, 0.01, 0.001$ and $b = 0.25, 0.5, 0.75, 1$. In general, we can see that the localization length is greater than in the previous case (i.e. figures 2(a) and (b)). However, in spite of the localization length increasing as the γ is decreased, only the zero frequency mode remains extended. In figure 2(f) we can see a finite size scaling of the localization length for $\gamma = 0.001$. Calculations indicate that only for $\omega = 0$ does the localization length diverge in proportion to the system size ($\lambda(\omega = 0) \propto N$). Some authors have considered ternary

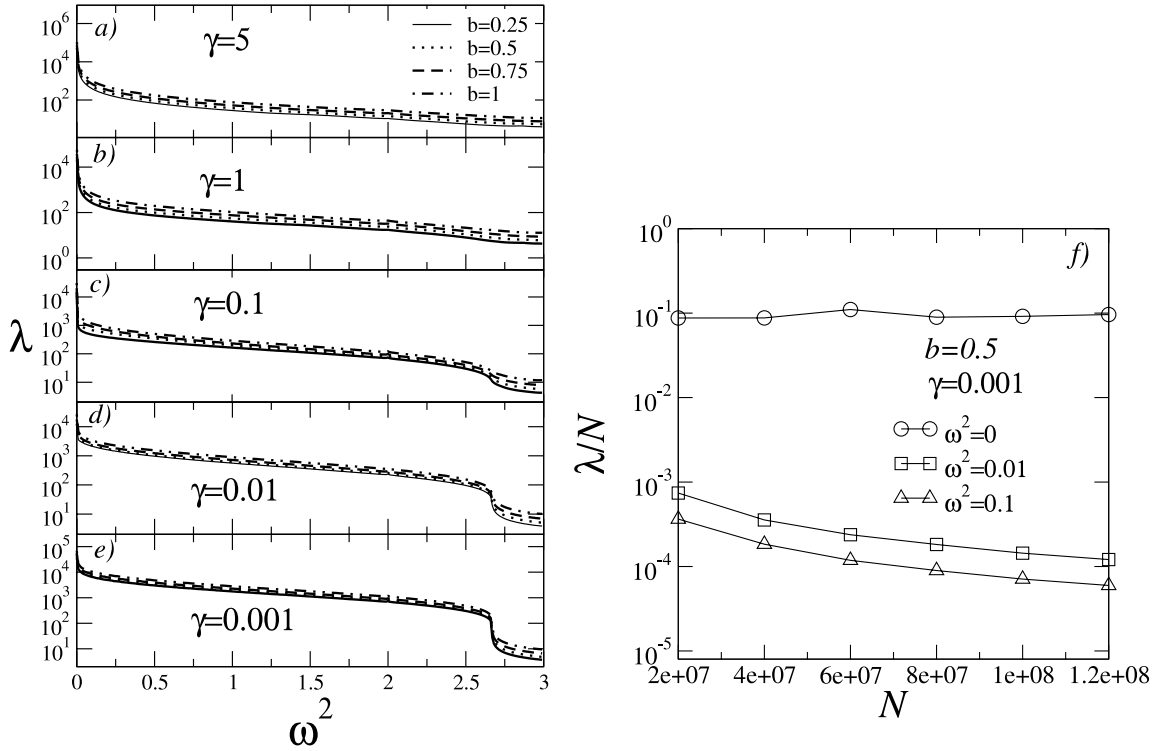


Figure 2. ((a)–(e)) Localization length λ versus ω^2 for a harmonic chain with an OU mass disordered distribution with $\gamma = 1$ (a), 5 (b), 0.1 (c), 0.01 (d) and 0.001 (e) and $b = 0.25, 0.5, 0.75$ and 1. (f) Finite size scaling of the localization length for $\gamma = 0.001, b = 0.5$ and $\omega^2 = 0, 0.01$ and 0.1. Calculations were made by using $N \approx 10^8$ and averaged over 100 disorder configurations. Our calculations indicate that for $\gamma \gg 0$ the harmonic chain considered here displays behavior similar to a harmonic chain with uncorrelated disorder distribution. We can see that the localization length increases as γ is decreased; however, only the zero frequency mode remains extended.

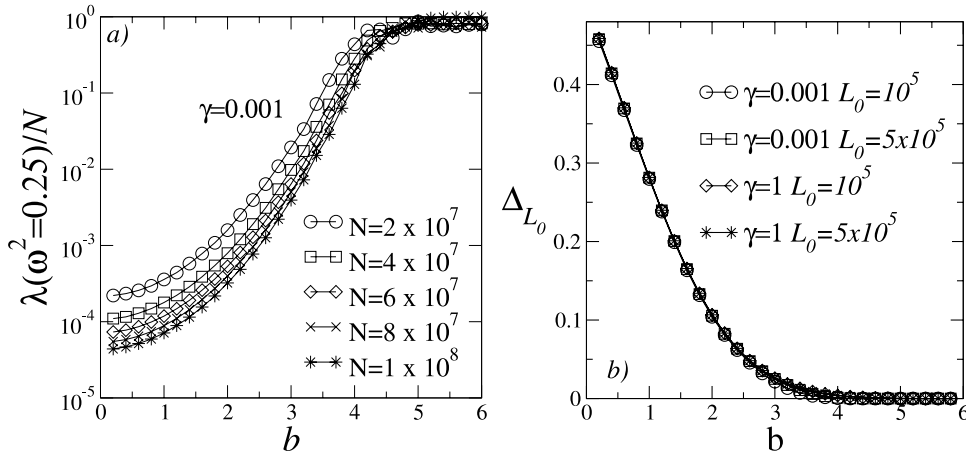


Figure 3. (a) Scaled localization length $\lambda(\omega^2=0.25)/N$ for $\omega^2 = 0.25$ versus b . Calculations were made for $\gamma = 0.001$ and system size $N = 2 \times 10^7$ to 10^8 masses. We can see clearly that for $b \leq 4$ the scaled localization length decreases as the system size increases, thus indicating localized states. For $b > 4$ the fine data collapse obtained indicates extended vibrational modes. (b) Numerical calculations of the local disorder strength in a segment with L_0 masses. For $b > 4$ the local disorder strength goes to zero; therefore, our calculations indicate that the apparent Anderson localization–delocalization transition obtained in (a) is, in fact, a disorder–order phase transition.

chains in the recent past [23–26]. In general, they obtained extended modes at the limit of large b . We will study here the possible appearance of extended states at the same limit. We will consider the nonzero frequency region. In figure 3(a) we show the scaled localization length λ/N for $\omega^2 = 0.25$ versus b . Calculations were made for $\gamma = 0.001$ and system size $N = 2 \times 10^7$ to 10^8 masses. We can see clearly that for

$b \leq 4$ the scaled localization length decreases as the system size increases, thus indicating localized states. For $b > 4$ we obtained a fine data collapse for the scaled localization length. This feature is a clear signature of extended vibrational modes. These results are in good agreement with previous calculations in [24–26] on the transport in ternary disorder distributions with strong long-range correlations. However,

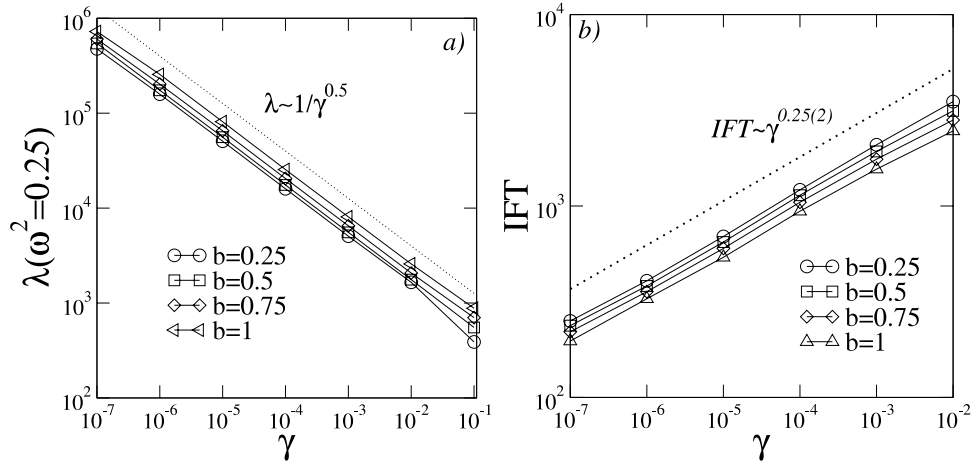


Figure 4. (a) Localization length λ versus γ for $b = 0.25, 0.5, 0.75$ and 1 . Our results indicate that the localization length scales in proportion to $\gamma^{0.5}$. (b) The effective amount of disorder in the chain calculated by using the integrated Fourier transform (*IFT*). Calculations of *IFT* versus γ were made for $b = 0.25, 0.5, 0.75$ and 1 and $N = 2^{26}$ masses. Our calculations indicate that $IFT \propto \gamma^{0.25(2)}$. The scaling behavior of the *IFT* associated with the well known dependence of λ on the amount of disorder corroborates the results obtained in (a) (i.e., $\lambda \propto 1/W^2 \propto 1/IFT^2 \propto 1/\gamma^{0.5}$).

her we will discuss these results by examining the intrinsic properties of the ternary sequence. We analyze some local properties of the ternary mass correlated disorder distribution. Let us compute the local standard deviation Δ_{L_0} of the mass distribution of a segment with L_0 masses. The local standard deviation Δ_{L_0} is defined by [28]

$$\Delta_{L_0} = \left(\sum_{k=1}^M \Delta_{k,L_0} \right) / M, \quad (13)$$

where

$$\Delta_{k,L_0} = \sqrt{ \sum_{n=(k-1)L_0+1}^{n=kL_0} (m_n)^2 / L_0 - \left(\sum_{i=(k-1)L_0+1}^{i=kL_0} m_n / L_0 \right)^2 }, \quad (14)$$

and $M = N/L_0$. Δ_{L_0} is a measurement of the local disorder strength in a segment with L_0 masses. In figure 3(b) we plot Δ_{L_0} versus b computed by using equations (13) and (14) in a ternary mass correlated disorder distribution with $\gamma = 0.001, 1$ and $N = 10^7$. Δ_{L_0} decreases substantially as the b parameter is increased. In particular, for $b > 4$ the local disorder strength goes to zero. Therefore, the existence of extended states for $b > 4$ is related to the decrease of the amount of disorder. Our results indicate that the phase transition obtained at about $b \approx 4$ is not an Anderson transition. For $b > 4$, the system becomes an ordered harmonic chain. In figure 4(a) we study the scaling of the localization length with the correlation degree γ . We show λ versus γ for $b = 0.25, 0.5, 0.75$ and 1 . Our results indicate that the localization length is proportional to $\gamma^{-0.5}$ within the range of γ used in our calculations ($\gamma = 10^{-7}$ to 0.1). We can understand this result by using an effective measure for the roughness of the mass distribution of our harmonic chain. Following [29, 30], we will consider the integrated Fourier transform (*IFT*) defined by $IFT =$

$\int_0^{k_{max}} m_k dk$, where m_k represents the Fourier transform of the mass distribution $\{m_n\}$. We can see that an uncorrelated random mass distribution with $\gamma \gg 0$ will have a large *IFT* due to its noise-like behavior. On the other hand, more regular structures with $\gamma \rightarrow 0$ will display a narrower Fourier spectrum and consequently a smaller *IFT*. In figure 4(b) we plot the *IFT* versus γ for $b = 0.25, 0.5, 0.75$ and 1 and $N = 2^{26}$ masses. Our calculations indicate that $IFT \propto \gamma^{0.25(2)}$. We can use the scaling behavior of the integrated Fourier transform (*IFT*) and scaling arguments to explain the divergence of the localization length with γ obtained in figure 4(a). It is well known that in a one-dimensional chain, the localization length diverges as $\lambda \propto 1/W^2$, where W is the degree of disorder. Since the integrated Fourier transform is a qualitative measurement of the disorder in the lattice, we can write $\lambda \propto 1/IFT^2 \propto 1/\gamma^{0.5}$, thus corroborating the scaling behavior obtained in figure 4(a).

3.2. Energy dynamics

We now show our results on the energy spread in this harmonic chain with Ornstein–Uhlenbeck correlated disorder. We will start by solving the Hamilton equations for an initial impulse excitation at the center of the chain (i.e. $P_n = \delta_{n,N/2}$ and $Q_n = 0$). The numerical solution was made by using the eighth-order Runge–Kutta method with time step $\Delta t = 0.005$ (see [31] for more detail). The energy conservation was checked to ensure numerical precision. In figures 5(a) and (b) we plot the scaled second moment $M_2(t)/t^{\kappa(\gamma)}$ as a function of time for $\gamma = 1, 0.1, 0.01$ and $0.001, b = 0.25$ and 0.5 and $N = 300\,000$ masses. We can see clearly that κ varies considerably with γ . For large values of γ we obtained exactly the same results as those expected for a harmonic chain with uncorrelated disorder, $\kappa \approx 1.5$ [15, 22, 21]. However, as the degree of correlation is increased (i.e., γ goes to zero) the energy spread becomes slower, with $\kappa < 1$. This sub-diffusive behavior is in contrast with the fast dynamics

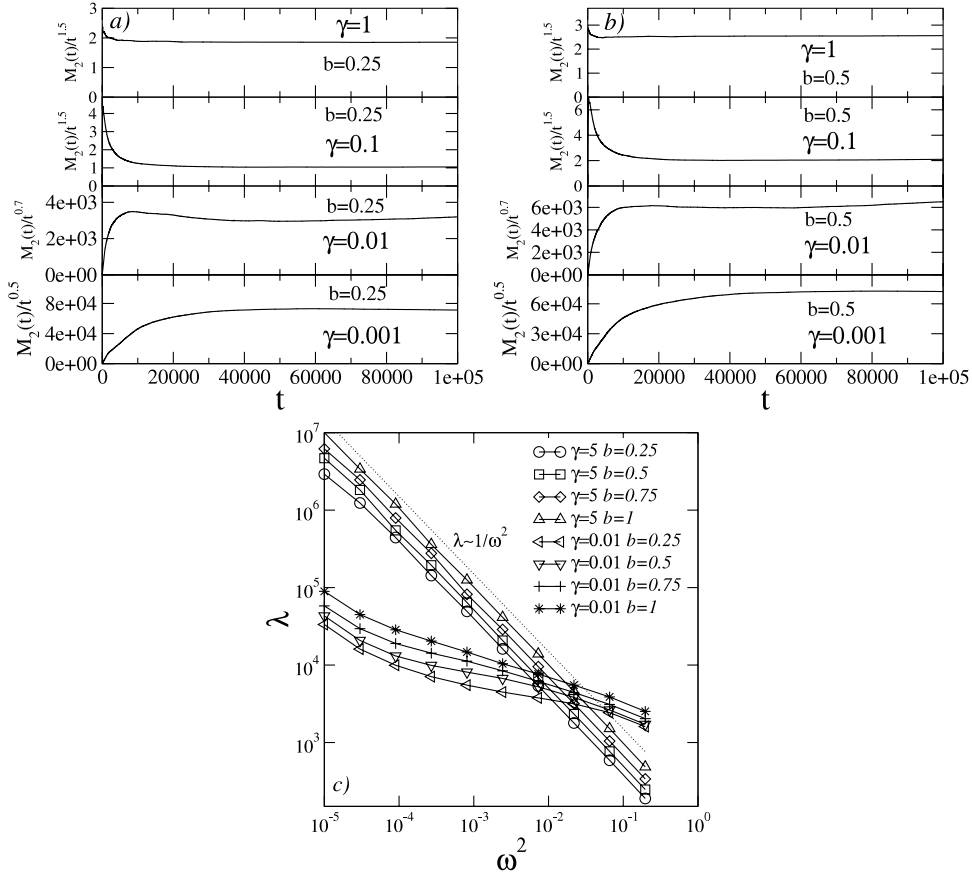


Figure 5. ((a), (b)) Scaled second moment $M_2(t)/t^{\kappa}$ as a function of time for $\gamma = 1, 0.1, 0.01$ and 0.001 , $b = 0.25$ and 0.5 and $N = 300\,000$ masses. The exponent of the second moment κ varies considerably with γ . For large γ we obtained exactly the same results as expected for a harmonic chain with uncorrelated disorder, $\kappa \approx 1.5$ [15, 22, 21]. However, as the degree of correlation is increased (i.e., γ goes to zero) the energy spread becomes slower, with $\kappa < 1$. To understand this slower dynamics even in the presence of correlation within the disorder distribution we will focus on the scaling behavior of the localization length around the resonance at the bottom of the band ($\omega = 0$). In (c) we plot the localization length versus ω at the bottom of the band. Calculations were made for $N = 10^8$ masses, $\gamma = 5$ and 0.01 and $b = 0.25, 0.5, 0.75$ and 1 . For $\gamma = 5$ we recover an uncorrelated random harmonic chain with $\lambda \propto \omega^{-2}$. This result is in good agreement with the super-diffusive behavior of the second moment, $M_2 \propto t^{1.5}$, found in (a) and (b). However, for $\gamma = 0.01$ we obtained a slow divergence for the localization length around $\omega = 0$, thus corroborating the slower dynamics obtained in (a) and (b) for $\gamma \rightarrow 0$.

found in [18–21]. The main issue behind this feature is the scaling of the localization length around the bottom of the band ($\omega = 0$). In [15] it was demonstrated that the spread of the energy in a disordered harmonic chain is strongly related to the number of extended modes. The number of free modes depends on the scaling of the localization length at the bottom of the band. The authors in [15] demonstrated that in a harmonic chain with an uncorrelated disorder distribution, the standard divergence $\lambda \propto 1/\omega^2$ promotes a super-diffusive behavior, $M_2 \propto t^{1.5}$. Furthermore, they also demonstrated that for a short-range dimer-like disorder distribution, the divergence of λ with ω becomes much faster and thus promotes a quasi-ballistic spread. Here, we have obtained the opposite trend. In figure 5(c) we plot the localization length versus ω at the bottom of the band. Calculations were made for $N = 10^8$ masses, $\gamma = 5$ and 0.01 and $b = 0.25, 0.5, 0.75$ and 1 . For $\gamma = 5$ we recover an uncorrelated random harmonic chain with $\lambda \propto \omega^{-2}$. This result is in good agreement with the super-diffusive behavior of the second moment, $M_2 \propto t^{1.5}$, found in figures 5(a) and (b). We can see clearly from figure 5(c) that for $\gamma = 0.01$ we obtained

a slower divergence for the localization length around $\omega = 0$. In fact, is not easy to estimate exactly the scaling behavior of λ with ω in the strongly correlated case; however, it is clearly slower than $1/\omega^2$. This result corroborates the sub-diffusive dynamics obtained in figures 5(a) and (b) for $\gamma \rightarrow 0$. In summary, in our calculations we have obtained numerical evidence contrasting with the super-diffusive spread that was reported in [15, 18–21]. We stress that by using analytical arguments it was demonstrated that a super-diffusive spread is obtained in harmonic chains and it is strongly dependent on the initial condition and the number of extended modes in the allowed frequencies band [15]. Furthermore, it was numerically demonstrated that the second moment of the energy distribution displays a super-diffusive dynamics even in two-dimensional nonperiodic harmonic lattices [20, 21]. In fact, the super-diffusive dynamics for an initial impulse excitation seems to be a universal feature of low-dimensional disordered harmonic lattices (it is found in both 1D and 2D). Therefore, in our calculations we have obtained new numerical evidence contrasting with these previous results. The key mechanism in our case is the number of eigenstates

around the low-frequency region, which is smaller than the number obtained in [18–21], thus corroborating the slower dynamics obtained in our model.

4. Summary

We have studied a one-dimensional ternary harmonic chain with the mass distribution constructed from an Ornstein–Uhlenbeck process. The ternary mass disordered distribution was generated from a mapping of the correlated Ornstein–Uhlenbeck process into a sequence of three different values. The probability of each value is controlled by a fixed parameter b . The degree of correlation in the Ornstein–Uhlenbeck process is controlled by the γ parameter. For large γ we recover an uncorrelated random sequence and for $\gamma \rightarrow 0$ the sequence displays long-range correlations. We have analyzed the localization properties of the above model by using basically two formalisms: numerical solution of the Hamilton equations and the transfer matrix formalism. We have obtained results that contradict previous results for models with ternary correlated sequences. Our results indicate that the correlated ternary mass distribution considered here does not promote the appearance of new extended modes. We have obtained an apparent Anderson transition for $b > 4$; however, by using calculations of the local disorder of the mass disorder distribution, we have numerically demonstrated that this model in fact displays a disorder–order transition for $b > 4$. In fact, the amount of disorder is vanishing at this limit. We would like to stress that a correct interpretation of the nature of the eigenstates at $b = 4$ for this type of model with ternary disorder was completely absent in the literature. We also calculated the scaling behavior of the localization length with the degree of correlation γ . By using a Fourier analysis we explained in detail the scaling behavior found ($\lambda \propto \gamma^{-0.5}$). In addition, we obtained the energy dynamics for this classical chain. Our results indicate that this kind of correlation promotes slower energy transport. We discussed this result based on the localization properties of the eigenstates at the bottom of the band. We anticipate that this work will stimulate further theoretical and experimental investigations along these lines.

Acknowledgments

This work was partially supported by CNPq, CAPES and FINEP (Federal Brazilian Agencies), CNPq-Rede Nanobioestruturas, as well as FAPEAL (Alagoas State Agency). F A B F de Moura would like to thank Earl Bellinger, Iram Gléria and Glauber T Silva for proofreading the manuscript. The research work of M O Sales is supported by a graduate program of CAPES.

References

- [1] Dean P 1964 *Proc. Phys. Soc.* **84** 727
Dean P 1972 *Rev. Mod. Phys.* **44** 127
- [2] Cressoni J C and Lyra M L 1996 *J. Phys.: Condens. Matter* **8** L83
- [3] Yan Y and Zhao H 2012 *J. Phys.: Condens. Matter* **24** 275401
- [4] Kundu A, Chaudhuri A, Roy D, Dhar A, Lebowitz J L and Spohn H 2010 *Europhys. Lett.* **90** 40001
- [5] Nika D L and Balandin A A 2012 *J. Phys.: Condens. Matter* **24** 233203
- [6] Li B, Zhao H and Hu B 2001 *Phys. Rev. Lett.* **86** 63
Dhar A 2001 *Phys. Rev. Lett.* **86** 5882
- [7] Garrido P L, Hurtado P I and Nadrowski B 2001 *Phys. Rev. Lett.* **86** 5486
Savin A V, Tsironis G P and Zolotaryuk A V 2002 *Phys. Rev. Lett.* **88** 154301
- [8] Dhar A 2002 *Phys. Rev. Lett.* **88** 249401
Garrido P L and Hurtado P I 2002 *Phys. Rev. Lett.* **88** 249402
- [9] Roy D and Dhar A A 2008 Statistical, nonlinear and soft matter physics *Phys. Rev. E* **78** 051112
- [10] Dhar Abhishek 2008 *Adv. Phys.* **57** 457
- [11] Shima H, Nishino S and Nakayama T 2007 *J. Phys.: Conf. Ser.* **92** 012156
- [12] Xiao J J, Yakubo K and Yu K W 2006 *Phys. Rev. B* **73** 054201
- [13] Xiao J J, Yakubo K and Yu K W 2006 *Phys. Rev. B* **73** 224201
- [14] Matsuda H and Ishii K 1970 *Prog. Theor. Phys. Suppl.* **45** 56
Ishii K 1973 *Prog. Theor. Phys. Suppl.* **53** 77
- [15] Datta P K and Kundu K 1995 *Phys. Rev. B* **51** 6287
- [16] Datta P K and Kundu K 1994 *J. Phys.: Condens. Matter* **6** 4465
- [17] Dominguez-Adame F, Macià E and Sánchez A 1993 *Phys. Rev. B* **48** 6054
- [18] de Moura F A B F, Coutinho-Filho M D, Raposo E P and Lyra M L 2003 *Phys. Rev. B* **68** 012202
- [19] Albuquerque S S, de Moura F A B F and Lyra M L 2005 *Physica A* **357** 165
- [20] de Moura F A B F and Domínguez-Adame F 2008 *Eur. Phys. J. B* **66** 165
- [21] de Moura F A B F 2010 *J. Phys.: Condens. Matter* **22** 435401
- [22] Wagner M, Zart G, Vazquez-Marquez J, Viliani G, Frizzera W, Pilla O and Montagna M 1992 *Phil. Mag. B* **65** 273
- [23] Carpena P, Galvan P B, Ivanov P Ch and Stanley H E 2002 *Nature* **418** 955
- [24] Esmailpour A, Cheraghchi H, Carpena P and Reza Rahimi Tabar M 2007 *J. Stat. Mech.* **P09014**
- [25] Lazo E and Diez E 2010 *Phys. Lett. A* **374** 3538
- [26] Lazo E and Diez E 2011 *Phys. Lett. A* **375** 2122
- [27] Gillespie D T 1996 *Phys. Rev. E* **54** 2084
- [28] Sales M O and de Moura F A B F 2012 *Physica E* **45** 97
- [29] Nascimento E M, de Moura F A B F and Lyra M L 2009 *Photon. Nanostruct. Fund. Appl.* **7** 101
- [30] Macià E 2006 *Rep. Prog. Phys.* **69** 397
- [31] Hairer E, Nørsett S P and Wanner G 2010 *Solving Ordinary Differential Equations I: Nonstiff Problems (Springer Series in Computational Mathematics)* (Berlin: Springer)
Press W H, Flannery B P, Teukolsky S A and Wetterling W T 2007 *Numerical Recipes: The Art of Scientific Computing* 3rd edn (New York: Cambridge University Press)